



PTPFCBBMA-*b*-PEG-*b*-PTPFCBBMA amphiphilic triblock copolymer: Synthesis and self-assembly behavior

Liang Tong^a, Zhong Shen^a, Dong Yang^b, Sheng Chen^c, Yongjun Li^a, Jianhua Hu^{b,**}, Guolin Lu^a, Xiaoyu Huang^{a,*}

^aKey Laboratory of Organofluorine Chemistry and Laboratory of Polymer Materials, Shanghai Institute of Organic Chemistry, Chinese Academy of Sciences, 345 Lingling Road, Shanghai 200032, PR China

^bKey Laboratory of Molecular Engineering of Polymers (Ministry of Education), Laboratory of Advanced Materials and Department of Macromolecular Science, Fudan University, 220 Handan Road, Shanghai 200433, PR China

^cR&D Center, Ciba (China) Ltd., Building 15, 99 Tianzhou Road, Shanghai 200233, PR China

ARTICLE INFO

Article history:

Received 13 February 2009

Received in revised form

23 March 2009

Accepted 30 March 2009

Available online 7 April 2009

Keywords:

ATRP

Block copolymer

Perfluorocyclobutyl aryl ether

ABSTRACT

We present the synthesis and self-assembly behavior of a new semi-fluorinated amphiphilic triblock copolymer. A series of perfluorocyclobutyl aryl ether-based amphiphilic ABA triblock copolymer containing hydrophilic poly(ethylene glycol) segment as the middle block were synthesized by atom transfer radical polymerization (ATRP). ATRP of 4-(4'-*p*-tolylxyperfluorocyclobutoxy)benzyl methacrylate was initiated by PEG-based bifunctional macroinitiators with different molecular weights to obtain the desired copolymers with narrow molecular weight distributions ($M_w/M_n \leq 1.30$) and the number of perfluorocyclobutyl linkage can be tuned by the feed ratio and the conversion of the fluorine-containing methacrylic monomer. The critical micelle concentrations of these amphiphilic ABA triblock copolymers in aqueous media were determined by fluorescence probe technique. They could aggregate to form spherical and cylindrical micelles visualized by TEM with varying the content of hydrophobic segment.

© 2009 Elsevier Ltd. All rights reserved.

1. Introduction

Fluoropolymers have many advantages compared with conventional carbon hydrogen polymer due to the incorporation of fluorocarbon functionality [1]; however, low solubility and processability limit their use. Thus, fluoropolymers including polychlorotrifluoroethylene, Teflon-AF, Cytop and various copolymers of poly-tetrafluoroethylene with low crystallinity have been modified to improve the processability [1]. Perfluorocyclobutyl (PFCB) aryl ether polymers are a relatively new class of fluoropolymers, which were developed by the researchers of Dow Chemical Co. in 1993 [2]. Recently, many new thermoplastic and thermoset PFCB polymers synthesized by thermal chain extension of bis- and tri-functionalized trifluorovinyl aryl ether monomers have been reported [3–5]. As an emerging class of semi-fluorinated polymers, PFCB-based polymers possess the common properties of fluoropolymer such as low surface energy, high thermal/oxidative stability and high chemical resistance;

moreover, they also provide many other advantages including optical transparency and improved processability [6–9].

Until now, only a few studies reported the synthesis of copolymers via trifluorovinyl aryl ether monomers and other commonly used monomers because of the normal high polymerization temperature (>150 °C) and unusual polymerization mechanism ($[2\pi + 2\pi]$ cycloaddition) compared to those of commercially available monomers [10–12]; furthermore, the number of PFCB linkage in copolymers was very difficult to be well controlled [10–13], which means the application of PFCB aryl ether polymer was certainly limited. Therefore, it is necessary to combine the high performance of PFCB aryl ether polymer with other commercial polymers for enlarging the application range of PFCB-based fluoropolymer.

Block copolymer with a stable covalent-bonded connection between two different segments may be a suitable choice to realize the above-mentioned concerns. In particular, much attention focused on the self-assembly behavior of amphiphilic block copolymer due to its potential exciting applications [14–17]. Block copolymers can be synthesized by the sequential feeding of different monomers via living radical polymerization [18–21] or the strategy of mechanism transformation via different polymerization methods [22–26]. Recent studies showed atom transfer

* Corresponding author. Tel.: +86 21 54925310; fax: +86 21 64166128.

** Corresponding author. Tel.: +86 21 55665280; fax: +86 21 65640293.

E-mail addresses: hujh@fudan.edu.cn (J. Hu), xyhuang@mail.sioc.ac.cn (X. Huang).

radical polymerization (ATRP) can be easily employed to synthesize amphiphilic block copolymers [27,28]. Especially, PEG-based macroinitiator prepared by converting the hydroxyl end group to halogen-containing ATRP initiation group can initiate ATRP of hydrophobic monomers to obtain different amphiphilic block copolymers containing hydrophilic PEG segment [29–31].

In this work, we present the synthesis and self-assembly behavior of the first example of amphiphilic triblock copolymer containing PFCB segment. A new monomer, 4-(4'-*p*-tolylxyperfluorocyclobutoxy)benzyl methacrylate (TPFCBBMA), was first prepared using commercially available 4-methylphenol as starting material, which incorporated PFCB linkage into methacrylic monomer as a side group. This monomer can be polymerized by ATRP in a controlled way to obtain well-defined homopolymer and the apparent polymerization rate exhibited first-order relation with respect to the concentration of monomer. Well-defined PTPFCBBMA-*b*-PEO-*b*-polychlorotrifluoroethylene PTPFCBBMA triblock copolymers with narrow molecular weight distributions were synthesized by ATRP of TPFCBBMA initiated by PEG-based bifunctional macroinitiators as shown in Scheme 1. Fluorescence spectroscopy and transmission electron microscopy (TEM) were used to study the self-assembly behavior of this kind of amphiphilic triblock copolymer.

2. Experimental section

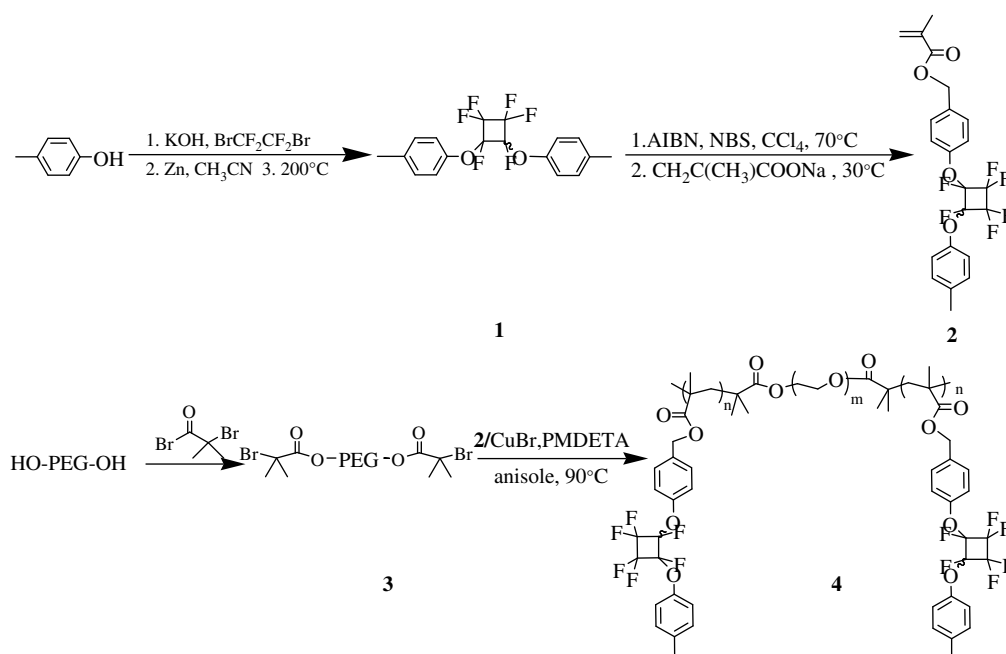
2.1. Materials

2,2'-Azobis(isobutyronitrile) (AIBN, Aldrich, 98%) was recrystallized from anhydrous ethanol. *N*-Phenyl-1-naphthylamine (PNA, Alfa Aesar, 97%) was purified by recrystallization in ethanol for three times. Granular zinc was activated by washing in 0.1 N HCl followed by drying at 140 °C *in vacuo* overnight. Copper (I) bromide (CuBr, Aldrich, 98%) was purified by stirring overnight over CH₃CO₂H at room temperature, followed by washing the solid with ethanol, diethyl ether and acetone prior to drying at 40 °C *in vacuo* for 1 day. Anisole (Aldrich, 99%) was dried over CaH₂ and distilled *in vacuo* prior to use. BrCF₂CF₂Br was prepared

by condensing equimolar amounts of bromine and tetrafluoroethylene at -195 °C cooled by liquid N₂ followed by warming up to 22 °C [32]. Poly(ethylene glycol) (PEG, *M_n* = 2000 and 4600 Aldrich, 99%), 4-methylphenol (Aldrich, 99%), methyl 2-bromopropionate (2-MBP, Aldrich, 99%), methacrylic acid (Aldrich, 99%), α -bromoisobutyryl bromide (Aldrich, 98%), dimethyl sulfoxide (DMSO, Aldrich, 99.9%), CCl₄ (Aldrich, 99.5%), *N*-bromosuccinimide (NBS, Aldrich, 99%), anisole (Aldrich, 99%) and *N,N,N',N',N'*-pentamethyldiethylenetriamine (PMDETA, Aldrich, 99%) were used as received.

2.2. Measurements

FT-IR spectra were recorded on a Nicolet AVATAR-360 FT-IR spectrophotometer with 4 cm⁻¹ resolution. All NMR analyses were performed on a Bruker Avance 500 spectrometer (500 MHz) in CDCl₃, TMS (¹H NMR) and CDCl₃ (¹³C NMR) were used as internal standards and CF₃CO₂H was used as external standard for ¹⁹F NMR. ESI-MS was measured by an Agilent LC/MSD SL system. Relative molecular weights and molecular weight distributions (*M_w*/*M_n*) were measured by a Waters gel permeation chromatography (GPC) system equipped with a Waters 1515 Isocratic HPLC pump, a Waters 2414 refractive index detector (RI) and a set of Waters Styragel columns (HR3, HR4 and HR5, 7.8 × 300 mm). GPC measurements were carried out at 35 °C using tetrahydrofuran (THF) as eluent with a flow rate of 1.0 mL/min. The system was calibrated with linear polystyrene standards. Conversions of TPFCBBMA were determined by GC using an HP 6890 system with SE-54 column. Steady-state fluorescent spectra of PNA were measured on a Hitachi FL-4500 spectrofluorometer with the band width of 5 nm for excitation and emission, the emission intensity at 418 nm was recorded to determine the *cmc* with a λ_{ex} = 340 nm. Glass transition temperature (*T_g*) was measured on a Perkin-Elmer Pyris 1 differential scanning calorimeter (DSC) under N₂ purge with a heating rate of 10 °C/min and determined from the second heating process after a quick cooling from 280 °C. TEM images were obtained using a Philips CM120 instrument operated at 80 kV.



Scheme 1. Synthesis of PTPFCBBMA-*b*-PEG-*b*-PTPFCBBMA amphiphilic triblock copolymer.

2.3. Preparation of dimer **1**

4-(4'-*p*-Tolyloxyperfluorocyclobutoxy)toluene **1** was obtained via thermal $[2\pi + 2\pi]$ cycloaddition of *p*-trifluorovinylxytoluene, which was prepared by fluoroalkylation of 4-methylphenol with $\text{BrCF}_2\text{CF}_2\text{Br}$ followed by Zn-mediated elimination with a total yield of 49.0% according to previous report [2]. The cycloaddition reaction was run at 200 °C in bulk and dimer **1** was obtained by silica column chromatography with a yield of 92.0%. ^1H NMR: δ (ppm): 2.33 (3H, CH_3), 7.01 (4H, $\text{C}_6\text{H}_4\text{CH}_3$), 7.12 (4H, $\text{C}_6\text{H}_4\text{-OC}_4\text{F}_6\text{O-C}_6\text{H}_4$). ^{13}C NMR: δ (ppm): 20.6 (CH_3), 105.0–115.2 (4C, PFCB), 118.3, 130.2, 135.0, 150.5. ^{19}F NMR: δ (ppm): –127.3 to –132.6 (6F, PFCB).

2.4. Synthesis of TPFCBBMA **2**

4-(4'-*p*-Tolyloxyperfluorocyclobutoxy)toluene **1** was brominated by NBS and AIBN in CCl_4 and the brominated product, 4-(4'-*p*-tolyloxyperfluorocyclobutoxy)-benzyl bromide, was obtained by silica column chromatography with a yield of 42.0%. Next, this brominated product reacted with sodium methacrylate in DMSO to give TPFCBBMA **2** with a yield of 57.6%. ESI-MS (m/z): calcd ($\text{M} + \text{Na}$)⁺ 483.1, found 483.1. FT-IR: ν (cm^{-1}): 3060, 2950, 1722, 1639, 1600, 1509, 1456, 1320, 1201, 1157, 1118, 963, 817. ^1H NMR: δ (ppm): 1.97 (3H, $\text{CH}_2=\text{C-CH}_3$), 2.33 (3H, $\text{C}_6\text{H}_4\text{CH}_3$), 5.17 (2H, $\text{C}_6\text{H}_4\text{CH}_2\text{O}$), 5.60, 6.16 (1H, $\text{CH}_2=\text{C-CH}_3$), 7.02 (2H, $\text{C}_6\text{H}_4\text{CH}_3$), 7.11 (4H, $\text{C}_6\text{H}_4\text{-OC}_4\text{F}_6\text{O-C}_6\text{H}_4$), 7.35 (2H, $\text{C}_6\text{H}_4\text{CH}_2\text{O}$). ^{13}C NMR: δ (ppm): 18.3 ($\text{CH}_2=\text{C-CH}_3$), 20.6 ($\text{C}_6\text{H}_4\text{CH}_3$), 65.6 ($\text{C}_6\text{H}_4\text{CH}_2\text{O}$), 105.0–115.2 (4C, PFCB), 118.3, 126.0 ($\text{CH}_2=\text{C-CH}_3$), 130.3, 134.9, 136.2 ($\text{CH}_2=\text{C-CH}_3$), 150.5, 167.2 (C=O). ^{19}F NMR: δ (ppm): –127.3 to –132.6 (6F, PFCB).

2.5. ATRP kinetics of TPFCBBMA **2**

ATRP of TPFCBBMA **2** was initiated by 2-MBP using PMDETA/CuBr as catalytic system in anisole. CuBr (0.0128 g, 0.089 mmol) was first added to a 10 mL Schlenk flask (flame-dried under vacuum prior to use) sealed with a rubber septum for degassing and kept under N_2 . Next, TPFCBBMA **2** (1.024 g, 2.23 mmol), PMDETA (37 μL , 0.178 mmol), 2-MBP (4.97 μL , 0.0445 mmol) and anisole (2.23 mL) were charged via a gas-tight syringe. The solution was degassed by three cycles of freezing–pumping–thawing and 0.40 mL of solution taken as the first data point (time = 0) was withdrawn from the flask using a gas-tight syringe. The flask was immersed into an oil bath thermostated at 90 °C to start the polymerization. At every time interval (1.0 h), 0.40 mL of solution was taken from the flask by a gas-tight syringe for ATRP kinetics study. The conversions of **2** were determined by GC. The molecular weights and molecular weight distributions were measured by GPC. This polymerization was terminated by immersing the flask into liquid nitrogen after 6 h. THF was added to the flask for dilution and the solution was filtered through a short Al_2O_3 column to remove the copper catalyst. The resulting solution was concentrated and precipitated into *n*-hexane. The raw product was purified by dissolving in THF and precipitating in *n*-hexane for three times and a white solid of PTPFCBBMA was finally obtained after drying *in vacuo*. Conversion of monomer **2**: 93.8%. GPC: $M_n = 31,400$, $M_w/M_n = 1.05$. T_g : 135.3 °C. FI-IR: ν (cm^{-1}): 3040, 2950, 1722, 1600, 1509, 1456, 1320, 1201, 1157, 1114, 963, 817. ^1H NMR: δ (ppm): 0.65, 0.89 (3H, CCH_3), 1.27, 1.61, 1.79 (CH_2C), 2.25 (3H, $\text{C}_6\text{H}_4\text{CH}_3$), 3.56 (3H, COOCH_3 of ATRP initiation group), 4.81 (2H, $\text{C}_6\text{H}_4\text{CH}_2\text{O}$), 6.94 (2H, $\text{C}_6\text{H}_4\text{CH}_3$), 7.03 (4H, $\text{C}_6\text{H}_4\text{-OC}_4\text{F}_6\text{O-C}_6\text{H}_4$), 7.20 (2H, $\text{C}_6\text{H}_4\text{CH}_2\text{O}$). ^{13}C NMR: δ (ppm): 20.1 (CH_3), 29.3 (CH_2C), 44.1 (CH_2C), 64.9 ($\text{C}_6\text{H}_4\text{CH}_2\text{O}$), 105.0–115.2 (4C, PFCB), 117.2, 129.2, 134.8, 149.3, 175.8 (C=O). ^{19}F NMR: δ (ppm): –127.3 to –132.6 (6F, PFCB).

2.6. Block copolymerization of TPFCBBMA **2**

Block copolymerization of TPFCBBMA **2** was initiated by PEG-based bifunctional macroinitiator **3** to provide well-defined PTPFCBBMA-*b*-PEG-*b*-PTPFCBBMA **4** triblock copolymer. PEG-based bifunctional macroinitiator **3** was prepared by treating PEG ($M_n = 2000$ and 4600) with 2-bromoisobutyryl bromide according to previous literature [33]. In a typical procedure, CuBr (14.4 mg, 0.1 mmol) and PEG-based bifunctional macroinitiator **3a** ($M_n = 2300$, $M_w/M_n = 1.08$, 120 mg, 0.05 mmol of ATRP initiation group) in 2 mL of anisole were first added to a 10 mL Schlenk flask (flame-dried under vacuum prior to use) sealed with a rubber septum under N_2 . After three cycles of evacuating and purging with N_2 , PMDETA (20.9 μL , 0.1 mmol) and TPFCBBMA **2** (0.92 g, 2.0 mmol) were introduced via a gas-tight syringe. The flask was degassed by three cycles of freezing–pumping–thawing followed by immersing the flask into an oil bath set at 90 °C. The polymerization was terminated by putting the flask into liquid nitrogen after 48 h. The reaction mixture was diluted with THF and passed through an alumina column to remove the copper catalyst. The solution was concentrated and precipitated into cold methanol. The final product, PTPFCBBMA-*b*-PEG-*b*-PTPFCBBMA **4c**, was obtained after drying *in vacuo* overnight. GPC: $M_n = 14,000$, $M_w/M_n = 1.18$. FI-IR: ν (cm^{-1}): 3040, 2962, 2954, 2885, 1735, 1605, 1506, 1452, 1322, 1267, 1196, 1157, 1112, 1018, 963, 817. ^1H NMR: δ (ppm): 0.68, 0.90 (3H, CCH_3), 1.25, 1.63, 1.78 (CH_2C), 2.25 (3H, $\text{C}_6\text{H}_4\text{CH}_3$), 3.64 (4H, $\text{OCH}_2\text{CH}_2\text{O}$), 4.84 (2H, $\text{C}_6\text{H}_4\text{CH}_2\text{O}$), 6.95 (2H, $\text{C}_6\text{H}_4\text{CH}_3$), 7.04 (4H, $\text{C}_6\text{H}_4\text{-OC}_4\text{F}_6\text{O-C}_6\text{H}_4$), 7.19 (2H, $\text{C}_6\text{H}_4\text{CH}_2\text{O}$). ^{13}C NMR: δ (ppm): 20.4 (CH_3), 30.4 (CH_2C), 44.6 (CH_2C), 66.1 ($\text{C}_6\text{H}_4\text{CH}_2\text{O}$), 70.8 (OCH_2), 106.0–115.8 (4C, PFCB), 117.9, 130.3, 135.0, 150.0, 175.5. ^{19}F NMR: δ (ppm): –127.3 to –132.6 (6F, PFCB).

2.7. Determination of critical micelle concentration

Acetone solution of PNA (1.15×10^{-3} mol/L) was added to a large amount of water until the concentration of PNA reached 6×10^{-7} mol/L. Different amounts of THF solutions of PTPFCBBMA-*b*-PEG-*b*-PTPFCBBMA **4** (10 mg/mL) were added to water containing PNA ($[\text{PNA}] = 6 \times 10^{-7}$ mol/L). All fluorescence spectra were recorded at 20 °C.

2.8. TEM images

Micelle solution was prepared by adding water to THF solution of block copolymer. PTPFCBBMA-*b*-PEG-*b*-PTPFCBBMA **4** triblock copolymer was first dissolved in THF with an initial concentration of 1 mg/mL. Next, de-ionized water was added slowly (0.36 mL/h) to 1 g of THF stock solution until the water content reached 35 wt%. The solution was sealed with a PTFE plug for equilibration under stirring for another 12 h. The solution was dialyzed against de-ionized water with slow stirring for 5 days to remove THF and de-ionized water was changed twice a day. For TEM studies, a drop of micellar solution was deposited on an electron microscopy copper grid coated with carbon film and the water evaporated at room temperature.

3. Results and discussion

3.1. Preparation of PFCB-linkage-containing methacrylic monomer

Traditional approach was first used to prepare *p*-trifluorovinylxytoluene in two steps from 4-methylphenol via fluoroalkylation with $\text{BrCF}_2\text{CF}_2\text{Br}$ followed by Zn-mediated elimination [2]. Next, 4-(4'-*p*-tolyloxyperfluorocyclobutoxy)toluene **1** was prepared by thermal cycloaddition of *p*-trifluorovinylxytoluene. The targeted

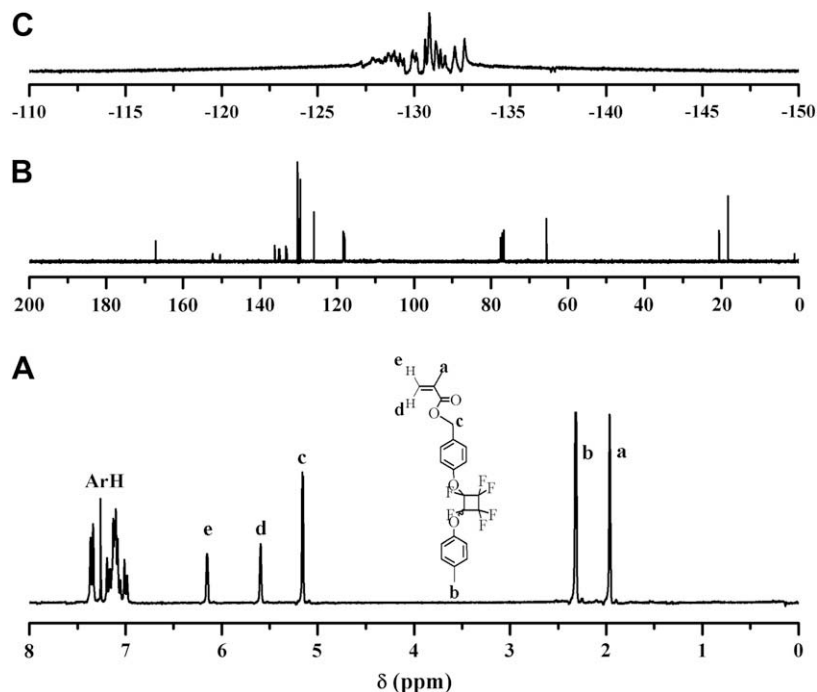


Fig. 1. ^1H NMR (A), ^{13}C NMR (B) and ^{19}F NMR (C) spectra of TPFBBMA **2**.

PFCB-linkage-containing methacrylic monomer was obtained via the esterification reaction between the mono-brominated product of dimer **1** and sodium methacrylate. FT-IR, ^1H NMR, ^{19}F NMR and ^{13}C NMR were employed to examine the chemical structure of monomer **2**. The peaks at 963, 1456, 1509 and 1600 cm^{-1} confirmed the successful incorporation of PFCB linkage. Typical signals of double bond and carbonyl were found to locate at 1639 and 1722 cm^{-1} , respectively. In addition, the sharp band centered at 817 cm^{-1} verified *para*-disubstituted benzene ring structure of PFCB aryl ether unit. Typical resonance signals of double bond appear at 5.60 and 6.16 ppm in ^1H NMR

spectrum of **2** as shown in Fig. 1A. The peaks at 7.02, 7.11 and 7.25 ppm corresponded to 8 protons of benzene ring in PFCB aryl ether unit. The resonance signals at 126.0 and 136.2 ppm in ^{13}C NMR spectrum of **2** (Fig. 1B) were attributed to 2 carbons of double bond. The peak at 167.2 ppm came from the carbon of carbonyl and a series of peaks ranging from 105.0 to 115.2 ppm represented 4 carbons of PFCB linkage. S series of peaks between -127.3 and -132.6 ppm in ^{19}F NMR spectrum of **2** (Fig. 1C) also demonstrated the existence of PFCB linkage. All the above results illustrated the successful synthesis of PFCB-containing monomer **2**.

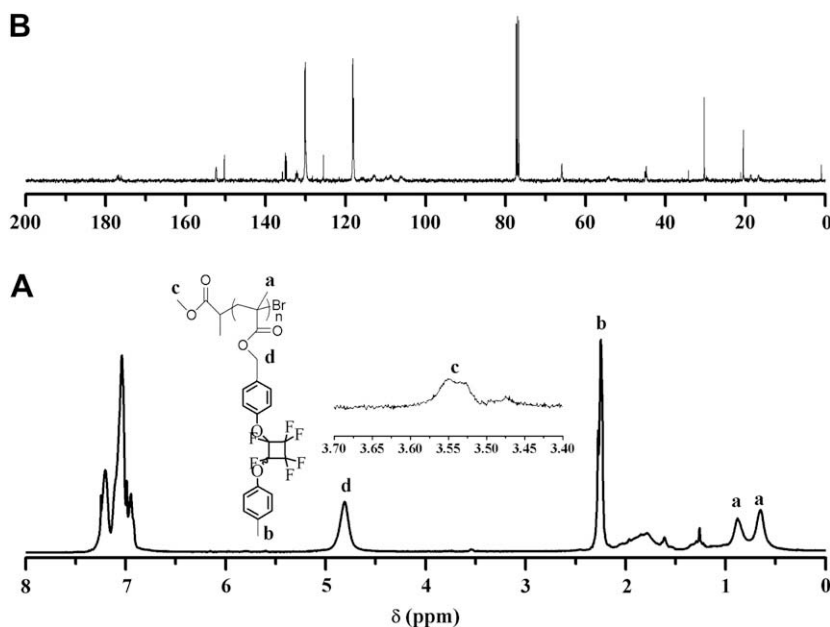


Fig. 2. ^1H NMR (A) and ^{13}C NMR (B) spectra of PTPFCBBMA homopolymer.

3.2. ATRP homopolymerization of TPFCBBMA 2

Well-defined PTPFCBBMA homopolymer with narrow molecular weight distribution ($M_w/M_n = 1.05$) was prepared via ATRP of monomer **2** in anisole using 2-MBP as initiator. The signals of double bond in ^1H NMR spectrum (Fig. 2A) disappeared after the homopolymerization. A minor peak at 3.56 ppm attributed to 3 protons of COOCH_3 in ATRP initiation group demonstrated ATRP mechanism. Furthermore, the existence of PFCB linkage in homopolymer was evidenced by the peaks between 105.0 and 115.2 ppm in ^{13}C NMR spectrum (Fig. 2B) and the peaks ranging from -127.3 to -132.6 ppm in ^{19}F NMR spectrum.

The semilogarithmic plot of $\ln([M]_0/[M])$ vs. time is depicted in Fig. 3A based on the data of conversions of TPFCBBMA **2** measured by GC, which shows the conversion of TPFCBBMA increases with the time and a linear dependence of $\ln([M]_0/[M])$ on the time when the feed ratio of TPFCBBMA to 2-MBP is 50:1. It is obvious that the apparent polymerization rate is first order with respect to the concentration of TPFCBBMA, illustrating a constant number of propagating species during the polymerization of TPFCBBMA. This phenomenon accorded with the characteristic of ATRP [34]. Fig. 3B shows the evolution of molecular weights and molecular weight distributions of homopolymer with the conversions of TPFCBBMA. The molecular weights increased linearly with the conversions of TPFCBBMA and the molecular weight distributions kept narrow during the polymerization ($M_w/M_n \leq 1.30$), which also matched the characteristics of ATRP [34]. Thus, it can be concluded that TPFCBBMA **2** can be polymerized by ATRP in a controlled way.

PTPFCBBMA has good solubility in common organic solvents including CH_2Cl_2 , chloroform, THF, DMSO and acetone; however, it is insoluble in water, which deemed PFCBBMA is a hydrophobic polymer. It was found PTPFCBBMA has a high decomposition temperature (T_d) around 320°C , indicating the excellent thermal stability of PTPFCBBMA. DSC curve shows this kind of polymethacrylate possesses a glass transition temperature (T_g) of 135°C , which is much higher than that of PMMA ($T_g = 100^\circ\text{C}$, $M_w = 57,000$) [35] due to the incorporation of PFCB aryl ether unit. This fact implies PFCB aryl ether unit can be introduced into methacrylic monomer to increase T_g for future application while keeping the transparency.

Table 1

Synthesis of PTPFCBBMA-*b*-PEG-*b*-PTPFCBBMA triblock copolymers.^a

| | Time (h) | M_n^d (g/mol) | M_w/M_n^d | cmc^e (g/mol) |
|-----------------------|----------|-----------------|-------------|------------------------|
| 4a^b | 12 | 6900 | 1.22 | 7.76×10^{-6} |
| 4b^b | 24 | 9400 | 1.15 | 4.81×10^{-6} |
| 4c^b | 48 | 14,000 | 1.18 | 2.51×10^{-6} |
| 4d^c | 12 | 8500 | 1.26 | 7.41×10^{-6} |
| 4e^c | 24 | 11,200 | 1.20 | 5.75×10^{-6} |
| 4f^c | 48 | 16,200 | 1.30 | 3.98×10^{-6} |

^a Initiated by PEG-based macroinitiator **3**, [2]:[Br group]:[CuBr]:[PMDETA] = 40:1:2:2.

^b Initiated by macroinitiator **3a** ($M_n = 2300$, $M_w/M_n = 1.08$).

^c Initiated by macroinitiator **3b** ($M_n = 4900$, $M_w/M_n = 1.09$).

^d Measured by GPC in THF.

^e Critical micelle concentration determined by fluorescence spectroscopy.

3.3. Synthesis of PTPFCBBMA-*b*-PEG-*b*-PTPFCBBMA triblock copolymer

PEG-based bifunctional macroinitiators were used to initiate ATRP of TPFCBBMA for synthesizing PTPFCBBMA-*b*-PEG-*b*-PTPFCBBMA triblock copolymers and the results were listed in Table 1. It is clear that all triblock copolymers' molecular weights were much higher than that of PEG-based macroinitiator, demonstrating the successful polymerization of TPFCBBMA. The molecular weights of triblock copolymers increased with the extending of polymerization time. Moreover, all triblock copolymers showed unimodal and symmetrical GPC curves with narrow molecular weight distributions ($M_w/M_n \leq 1.30$), indicating that intermolecular coupling reactions could be neglected [36].

PTPFCBBMA-*b*-PEG-*b*-PTPFCBBMA **4** triblock copolymer was characterized by FT-IR, ^1H NMR, ^{13}C NMR and ^{19}F NMR, respectively. Fig. 4A shows FT-IR spectrum of PTPFCBBMA-*b*-PEG-*b*-PTPFCBBMA **4**. The signal of double bond was found to disappear and the sharp peak of carbonyl still appeared at 1735 cm^{-1} . The presence of PFCB aryl ether unit was affirmed by the bands at 817, 963, 1452, 1506 and 1605 cm^{-1} and the peaks at 1112 and 1018 cm^{-1} illustrated the incorporation of PEG segment, which are similar to those of PTPFCBBMA **2** homopolymer and PEG-based macroinitiator **3** as shown in Fig. 4B and C, respectively. ^1H NMR spectrum of PTPFCBBMA-*b*-PEG-*b*-PTPFCBBMA **4** is shown in Fig. 5A. The peaks

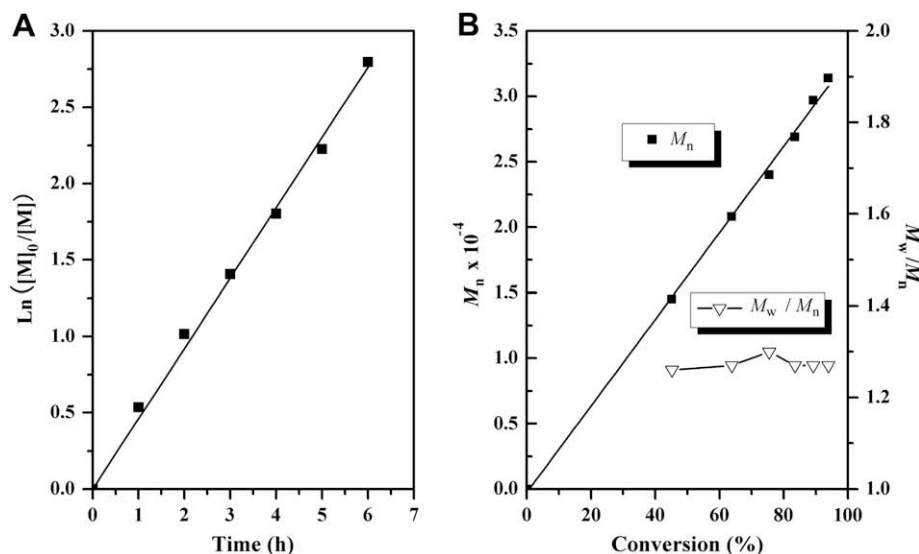


Fig. 3. (A) Kinetic plot for solution ATRP of TPFCBBMA **2**. (B) Dependence of molecular weight (M_n) and molecular weight distribution (M_w/M_n) on the conversion of monomer for solution ATRP of TPFCBBMA **2**.

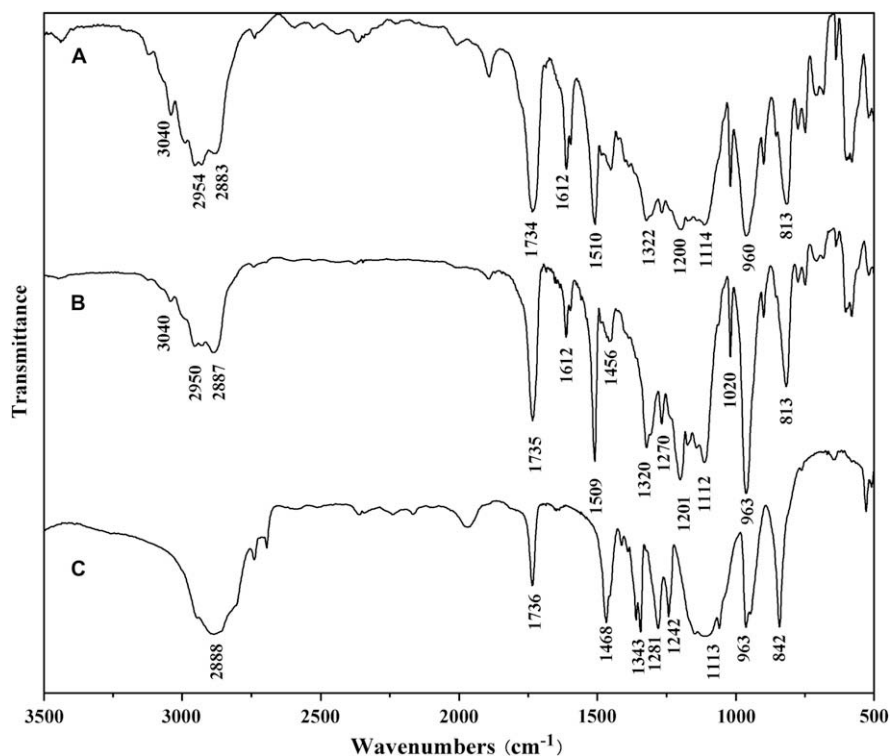


Fig. 4. FT-IR spectra of PTPFCBBMA-*b*-PEG-*b*-PTPFCBBMA **4** (A), PTPFCBBMA **2** (B) and PEG-based macroinitiator **3**.

at 6.94, 7.03 and 7.20 ppm were attributed to 8 protons of PFCB aryl ether unit. The signal at 3.64 ppm corresponded to 4 protons of OCH_2CH_2 repeating units of PEG block. Since double bonds disappeared after ATRP block copolymerization, the peak of 2 protons

of $\text{C}_6\text{H}_4\text{CH}_2\text{O}$ group moved to 4.84 ppm compared to that appeared at 5.17 ppm before copolymerization as shown in Fig. 1A. Furthermore, both a series of peaks ranging from 106.0 to 115.8 ppm in ^{13}C NMR spectrum (Fig. 5B) and the signals between -127.3 and

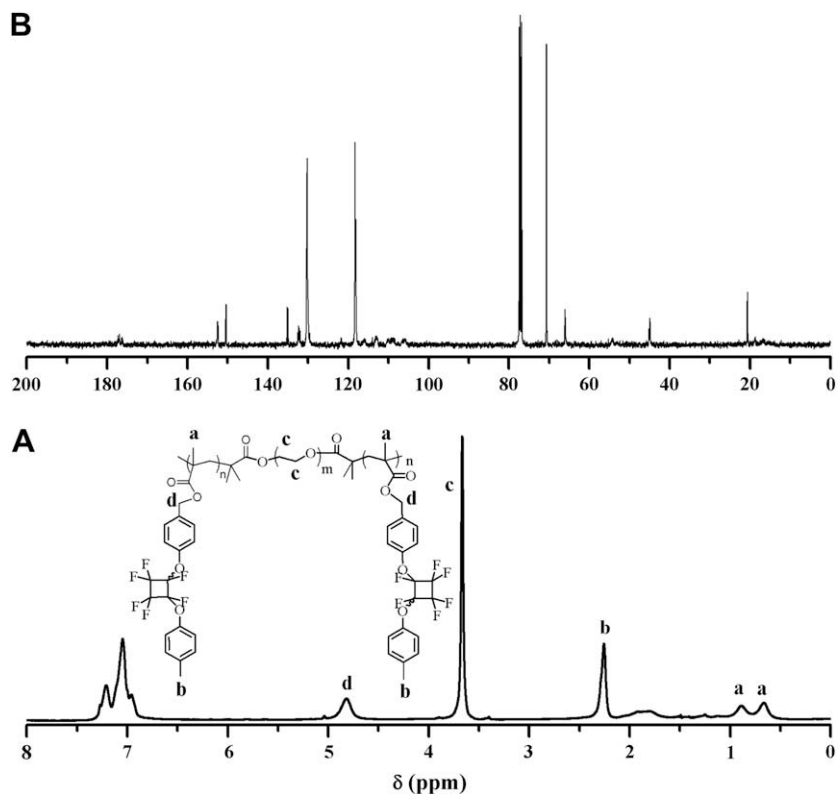


Fig. 5. ^1H NMR (A) and ^{13}C NMR (B) spectra of PTPFCBBMA-*b*-PEG-*b*-PTPFCBBMA **4** in CDCl_3 .

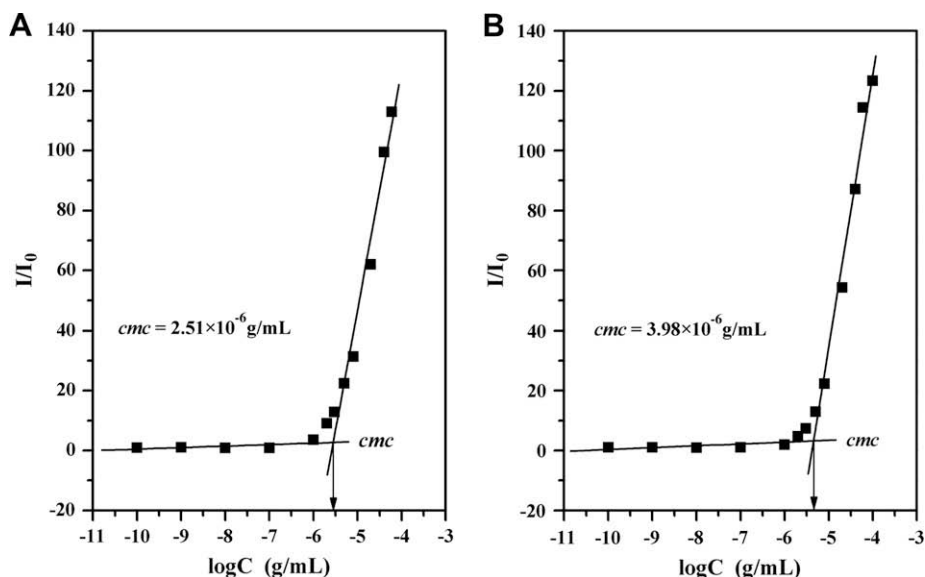


Fig. 6. Dependence of fluorescence intensity ratio of PNA emission band at 418 nm on the concentration of PTPFCBBMA-*b*-PEG-*b*-PTPFCBBMA **4c** and **4f**.

–132.6 ppm in ^{19}F NMR spectrum verified the existence of PFCB aryl ether unit. From the above-mentioned results, the chemical structure of PTPFCBBMA-*b*-PEG-*b*-PTPFCBBMA **4** triblock copolymer can be confirmed.

3.4. Self-assembly of PTPFCBBMA-*b*-PEG-*b*-PTPFCBBMA triblock copolymer

In this case, fluorescence technique was used to examine the *cmc* value of PTPFCBBMA-*b*-PEG-*b*-PTPFCBBMA **4** amphiphilic triblock copolymer in aqueous media with PNA as probe. PNA can display higher fluorescence activity in nonpolar surroundings and

its fluorescence can be very easily quenched by polar solvents such as water; moreover, it is a more suitable fluorescent probe than pyrene in terms of reproducibility [37]. The relationships of fluorescence intensity ratio (I/I_0) of PNA as a function of the concentration of PTPFCBBMA-*b*-PEG-*b*-PTPFCBBMA **4c** and **4f** at 20 °C are shown in Fig. 6A and B, respectively. The ratios were almost constant while the concentration of triblock copolymer was below a certain value; however, I/I_0 increased sharply when the concentration was higher than that value, showing the incorporation of PNA probe into the hydrophobic region of micelles. Thus, *cmc*s of copolymers **4c** and **4f** were determined to be the intersections of 2 straight lines with values of

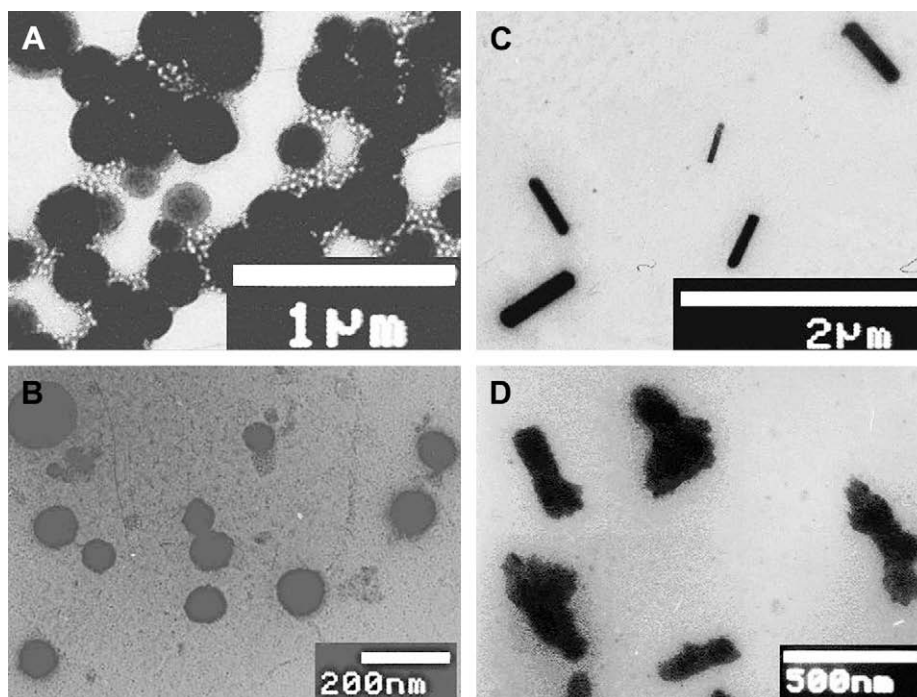


Fig. 7. TEM images of micelles formed by PTPFCBBMA-*b*-PEG-*b*-PTPFCBBMA **4a** (A), **4c** (B), **4d** (C) and **4f** (D) in pure water, initial concentration of copolymer in THF: 1 mg/mL.

2.51×10^{-6} g/mL and 3.98×10^{-6} g/mL, respectively. The *cmc* values of PTPFCBBMA-*b*-PEG-*b*-PTPFCBBMA **4** triblock copolymers (Table 1) are all around 10^{-6} g/mL, which are much lower than those of low molecular weight surfactants; however, they are comparable with those of polymeric amphiphiles [38–41]. In addition, these values decreased with the increasing of molecular weights because of the raising of the contents of hydrophobic PTPFCBBMA segment.

PTPFCBBMA-*b*-PEG-*b*-PTPFCBBMA **4** is difficult to dissolve in water due to the relative high content of hydrophobic PTPFCBBMA unit. Therefore, dialysis method was employed to prepare micelles, PTPFCBBMA-*b*-PEG-*b*-PTPFCBBMA **4** was first dissolved in small amount of THF followed by adding water (selective solvent for PEG) dropwise to induce self-assembly and THF was removed by dialysis against de-ionized water with slow stirring [42]. Micellar morphologies were directly visualized under TEM. Fig. 7 show micellar morphologies formed by **4** with different molecular weights in pure water when the initial concentration of copolymer in THF was 1 mg/mL. PTPFCBBMA-*b*-PEG-*b*-PTPFCBBMA **4a** synthesized from macroinitiator **3a** aggregated to form spherical micelles (ca. 250 nm) as shown in Fig. 7A. When the block length ratio of PEG to PTPFCBBMA decreases with a fixed length of hydrophilic PEG block, Fig. 7B showed **4c** associated into cylinders (diameter: ca. 100 nm and length: ca. 450 nm). The observed phenomenon is similar to a previous report on the system of PS-*b*-PAA, in which spherical aggregates turned to cylindrical micelles as the block length ratio of hydrophilic PAA segment to hydrophobic PS segment decreased [43]. PTPFCBBMA-*b*-PEG-*b*-PTPFCBBMA **4** triblock copolymers synthesized from macroinitiator **3b** also have the similar trend. With the increasing of molecular weights, spherical micelles (ca. 100 nm) formed by PTPFCBBMA-*b*-PEG-*b*-PTPFCBBMA **4d** with shorter PTPFCBBMA blocks (Fig. 7C) turned to cylindrical micelles (diameter: ca. 150 nm and length: ca. 400 nm) aggregated by **4f** with longer PTPFCBBMA segments (Fig. 7D). For the sphere, the core radius has to increase together with the raising of the content of hydrophobic PTPFCBBMA segments, indicating the stretching degree of PTPFCBBMA segments should also increase which is thermodynamically unfavorable. For the cylinder, the additional freedom degree along the axis made many chains incorporate into the structure without remarkable changes in their original conformation [43]. As a result, spherical aggregates transformed into cylindrical micelles while the length of hydrophobic PTPFCBBMA block increased. Thus, it can be concluded that the content of hydrophobic PTPFCBBMA block played an important role in determining micellar morphologies.

4. Conclusion

In summary, the first example of ABA amphiphilic triblock copolymer containing PFCB segment was reported. A new methacrylic monomer possessing PFCB linkage as a side group was prepared in 5 steps using commercially available 4-methylphenol as starting material, which can be polymerized by ATRP in a controlled way with a type of first-order kinetics. PTPFCBBMA homopolymer shows excellent thermal properties with high T_g and T_d , and excellent solubility in common organic solvents. ATRP of PTPFCBBMA was initiated by PEG-based bifunctional macroinitiator to synthesize PTPFCBBMA-*b*-PEG-*b*-PTPFCBBMA amphiphilic triblock copolymers. These triblock copolymers can self-assemble in water with *cmc* value around 10^{-6} g/mL. Spherical micelles were formed with shorter hydrophobic block and they turned to cylindrical micelles with the increasing of the content of hydrophobic PTPFCBBMA segment.

Acknowledgement

The authors thank the financial support from National Natural Science Foundation of China (20674094 and 50873029), Ministry of Science and Technology of “National High Technology Research and Development Program” (2006AA03Z541), Shanghai Rising Star Program (07QA14066) and Shanghai Scientific and Technological Innovation Project (08431902300).

References

- [1] Babb DA, Snelgrove RV, Smith DW, Mudrich SF. Step-growth polymers for high-performance materials. Washington, DC: American Chemical Society; 1996. pp. 431–41.
- [2] Babb DA, Ezzell BR, Clement KS, Richey WF, Kennedy AP. J Polym Sci Part A Polym Chem 1993;31:3465–77.
- [3] Jin J, Topping CM, Chen S, Ballato J, Foulger SH, Smith DW. J Polym Sci Part A Polym Chem 2004;42:5292–300.
- [4] Smith DW, Boone HW, Traiphol R, Shah H, Perahia D. Macromolecules 2000;33:1126–8.
- [5] Ghim J, Shim HS, Shin BG, Park JH, Hwang JT, Chun C, et al. Macromolecules 2005;38:8278–84.
- [6] Feiring AE. Fluoroplastics. In: Banks RE, Smart BE, Tatlow JC, editors. Organofluorine chemistry: principle and commercial applications. New York: Plenum Press; 1994. p. 339–71.
- [7] Yamabe M. Fluoropolymer coatings. In: Banks RE, Smart BE, Tatlow JC, editors. Organofluorine chemistry: principle and commercial applications. New York: Plenum Press; 1994. p. 397–402.
- [8] Resnick PR, Buck WH. Teflon® AF amorphous fluoropolymers. In: Schirs J, editor. Modern fluoropolymers: high performance polymers for diverse applications. New York: Wiley; 1997. p. 397–420.
- [9] Iacono ST, Budy SM, Jin JY, Smith DW. J Polym Sci Part A Polym Chem 2007;45:5705–21 and references therein.
- [10] Lu GL, Zhang S, Huang XY. J Polym Sci Part A Polym Chem 2006;44:5438–44.
- [11] Huang XY, Lu GL, Peng D, Zhang S, Qing FL. Macromolecules 2005;38:7299–305.
- [12] Zhu YQ, Huang YG, Meng WD, Li HQ, Qing FL. Polymer 2006;47:6272–9.
- [13] Souzy R, Ameduri B, Boutevin B. Prog Polym Sci 2004;29:75–106.
- [14] Park M, Harrison C, Chaikin PM, Register RA, Adamson DH. Science 1997;276:1401–4.
- [15] Lee JS, Hirao A, Nakahama S. Macromolecules 1988;21:274–6.
- [16] Widawski G, Rawiso M, Franois B. Nature 1994;369:387–9.
- [17] Patel NP, Spontak RJ. Macromolecules 2004;37:2829–38.
- [18] Lligadas G, Ladislav JS, Guliasvili T, Percec V. J Polym Sci Part A Polym Chem 2008;46:278–88.
- [19] Moad G, Rizzardo E, Thang SH. Polymer 2008;49:1079–131.
- [20] Mueller L, Jakubowski W, Tang W, Matyjaszewski K. Macromolecules 2007;40:6464–72.
- [21] Uchiike C, Terashima T, Ouchi M, Ando T, Kamigaito M, Sawamoto M. Macromolecules 2007;40:8658–62.
- [22] Bernaerts KV, Du Prez FE. Prog Polym Sci 2006;31:671–722.
- [23] Yagci Y, Atilla TM. Prog Polym Sci 2006;31:1133–70.
- [24] Breland LK, Murphy JC, Storey RF. Polymer 2006;47:1852–60.
- [25] Coca S, Paik HJ, Matyjaszewski K. Macromolecules 1997;30:6513–6.
- [26] Hizal G, Yagci Y, Schnabel W. Polymer 1994;35:4443–8.
- [27] Neugebauer D, Zhang Y, Pakula T, Matyjaszewski K. Polymer 2003;44:6863–71.
- [28] Lee SB, Russell AJ, Matyjaszewski K. Biomacromolecules 2003;4:1386–93.
- [29] Cao HQ, Lin WR, Liu AH, Zhang J, Wan XH, Zhou QF. Macromol Rapid Commun 2007;28:1883–8.
- [30] Jiang XZ, Luo SZ, Armes SP, Shi WF, Liu SY. Macromolecules 2006;39:5987–94.
- [31] Jiang JQ, Tong X, Zhao Y. J Am Chem Soc 2005;127:8290–1.
- [32] Katsuhara Y, DesMatteau DD. J Am Chem Soc 1980;102:2681–6.
- [33] Jankova K, Chen XY, Kops J, Batsberg W. Macromolecules 1998;31:538–41.
- [34] Wang JS, Matyjaszewski K. J Am Chem Soc 1995;117:5614–5.
- [35] Kuo SW, Kao HC, Chang FC. Polymer 2003;44:6873–82.
- [36] Cheng G, Boker A, Zhang M, Krausch G, Muller AHE. Macromolecules 2001;34:6883–8.
- [37] Xu PS, Tang HD, Li SY, Ren J, Van Kirk E, Murdoch WJ, et al. Biomacromolecules 2004;5:1736–44.
- [38] Clendenning SB, Fournier-Bidoz S, Pietrangelo A, Yang GC, Han SJ, Brodersen PM, et al. J Mater Chem 2004;14:1686–90.
- [39] Whitesides GM, Grzybowski B. Science 2002;295:2418–21.
- [40] Ruokolainen J, Makinen R, Torkkeli M, Makela T, Serimaa R, Rinke GT, et al. Science 1998;280:557–60.
- [41] Thurmond KB, Kowalewski T, Wooley KL. J Am Chem Soc 1997;119:6656–65.
- [42] Bhargava P, Zheng JX, Li P, Quirk RP, Harris FW, Cheng SZD. Macromolecules 2006;39:4880–8.
- [43] Zhang LF, Eisenberg A. J Am Chem Soc 1996;118:3168–81.